Published in final edited form as:
Biochem J. 2011 October 1; 439(1): 45–55. doi:10.1042/BJ20110274.

Autotaxin induces lung epithelial cell migration through lysoPLD activity-dependent and -independent pathways

Jing Zhao[1], **Donghong He**[2], **Evgeny Berdyshev**[3], **Mintao Zhong**[1], **Ravi Salgia**[4], **Andrew J. Morris**[5], **Susan S. Smyth**[5], **Viswanathan Natarajan**[2,3,¶], and **Yutong Zhao**[1,¶]

[1]Department of Medicine, University of Pittsburgh School of Medicine, Pittsburgh, PA

[2]Department of Pharmacology, University of Illinois at Chicago, Chicago, IL

[3]Department of Medicine, University of Illinois at Chicago, Chicago, IL

[4]Department of Medicine, The University of Chicago, Chicago, IL

[5]Department of Medicine, University of Kentucky, Lexington, KY.

SYNOPSIS

Lung cell migration is a crucial step for re-epithelialization that in turn is essential for remodeling and repair after lung injury. We hypothesize that secreted autotaxin (ATX), which exhibits lysophospholipase D (lysoPLD) activity, stimulates lung epithelial cell migration through lysophosphatidic acid (LPA) generation-dependent and -independent pathways. Release of endogenous ATX protein and activity was detected in lung epithelial cell culture medium. ATX with V5 tag (ATX-V5) overexpressed conditional medium had higher LPA levels compared to control medium and stimulated cell migration through $G_{\alpha i}$-coupled LPA receptors, cytoskeleton rearrangement, phosphorylation of PKCδ and cortactin at the leading edge of migrating cells. Inhibition of PKCδ attenuated ATX-V5 overexpressed conditional medium-mediated phosphorylation of cortactin. In addition, a recombinant ATX mutant, lacking lysoPLD activity, or heat-inactived ATX also induced lung epithelial cell migration. Extracelluar ATX bound to LPA receptor and integrin β4 complex on A549 cell surface. Finally, intratracheal administration of lipopolysaccharide into mouse airway induced ATX release and LPA production in bronchoalveolar lavage fluid. These results suggested a significant role for ATX in lung epithelial cell migration and remodeling through its ability to induce LPA production-mediated phosphorylation of PKCδ and cortactin. In addition we also demonstrated assocation of ATX with epithelial cell surface LPA receptor and integrin β4.

Keywords

ATX (autotoxin); lysoPLD; LPA; cell migration; signal transduction

INTRODUCTION

Lung epithelium functions as a physical barrier between the air and interstitium of the lung. In respiratory lung diseases, injury to the lung epithelial lining leads to inflammation and

Address correspondence to: Yutong Zhao, MD, PhD. Department of Medicine, University of Pittsburgh School of Medicine, 3459 Fifth Ave NW 628, MUH Pittsburgh, PA, 15213 Tel: 412-648-9488 zhaoy3@upmc.edu.
¶Co-Senior Authors of this work

The authors declare no conflicts of interest

invasion of inhaled stimuli into lung interstitium [1-3]. Lung epithelial cell migration after injury is an important step for re-epithelialization, wound healing, and restoring lung function [4-6]. For example, epithelial cell migration is a key feature of the repair process after septic (lipopolysaccharide, LPS)-induced lung injury [7]. The underlying molecular mechanisms of cell migration have been studied in variety of cell types, including alveolar epithelial cells [8-10]. Cortactin, an actin-associated scaffolding protein, localizes to the edges of lamellipodia and filopodia of spreading or migrating cells, and tyrosine phosphorylation of cortactin regulates cortactin-mediated cell motility and migration [11-13]. Tyrosine phosphorylation of cortactin by Src kinase [11, 14] is regulated by PKC isoforms [15-18]. PKCδ levels are increased 3-fold in the highly metastatic mammalian tumor cells MTLn3 compared to relatively less metastatic cell lines and inhibition of PKCδ reduced cell migration and lung metastasis [19]. Furthermore, PKCδ-induced polymerization of actin requires its interaction with cortactin [20].

Accumulating evidence suggests that autotaxin (ATX), a tumor cell motility-stimulating factor, induces cell motility and tumor metastasis [21-24]. Originally isolated from melanoma cell supernatant [23], ATX has lysophospholipase D (lysoPLD) activity, and catalyzes the hydrolysis of lysophosphatidylcholine (LPC) to lyosphosphatidic acid (LPA) [25-27]. LPA present at nano- to micro-molar concentrations in various biological fluids [28-30] induces cell proliferation, migration, and cytokine release through binding to G-protein-coupled LPA-receptors on cell surface. [22, 24, 25, 31-33]. The effect of ATX on tumor cell motility is dependent on levels of LPA generated and type(s) of LPA receptors involved in the transmission of signal [21, 22, 25-27]. Recent studies have shown that ATX interacts with lymphocytes and activated platelets in a β3-integrin-dependent manner, which could serve to localise LPA production to the cell surface or maybe a new mechanism for ATX to regulate cell motility in a lysoPLD activity independent manner [34]. ATX is expressed in lung epithelial cells [35], and inhibition of ATX attenuates lung cancer cell migration [24]. ATX secretion is necessary for this activity; however, the intracellular molecular pathway whereby secreted ATX regulates migration of this cell type are unclear.

We demonstrated here that the secreted ATX induced lung epithelial cell migration through both LPA generation-dependent and -independent mechanisms. We identified a new ATX effector pathway underscored by PKCδ-mediated phosphorylation of cortactin regulated ATX-induced cell migration. Our results also showed for the first time that extracellular ATX interacted with LPA receptor and integrin β4 complex on the cell surface. The potential biological significance of these findings are evidenced by our demonstration that ATX and LPA levels are increased in bronchoalveolar lavage (BAL) fluid in a murine model of LPS-induced acute lung injury. Taken together, these results suggested a novel role of ATX in lung re-epithelialization and remodeling after injury.

EXPERIMENTAL PROCEDURES

Materials

1-oleoyl (18:1) LPA, ki16425, and antibody to β-actin were purchased from Sigma-Aldrich (St. Louis, MO). Brp-LPA and FS-3 were procured from Echelon Inc. (Salt lake city, UT). Egg lysoPC was from Avanti Polar Lipids, Inc (Alabaster, AL). Antibodies to p-cortactin and PKCδ were obtained from Cell Signaling Technology (Beverly, MA). Antibodies to LPA_1 and ATX were from Lifespan Bioscience (Seattle, WA). Antibodies to V5 tag, cortactin, scrambled, autotoxin, and LPA_1 siRNAs were purchased from Santa Cruz Biotechnology (Santa Cruz, CA). Antibody to phospho-tyrosine was from Zymed laboratories (San Franciso, CA). Horseradish peroxidase-conjugated goat anti-rabbit, anti-mouse were obtained from Bio-Rad Laboratories (Hercules, CA). ECL kit for detection of proteins by Western blotting was obtained from Thermo Fisher Scientific (Waltham, MA).

Alexa Fluor-488 goat anti-rabbit, and Alexa Fluor-549 chicken anti-goat antibodies were purchased from Molecular Probes (Eugene, OR, U.S.A.). All other reagents were of analytical grade.

Cell culture

A549 cells and primary human small airway epithelial cells (HSAEpCs) were purchased from American Type Cell Culture (Manassas, VA). A549 cells were cultured in RPMI 1640 medium (Lonza, Walkersville, MD) containing 10% fetal bovine serum (FBS), penicillin (100 U/ml) and streptomycin (100 μg/ml) at 37°C in 5% CO_2. HSAEpCs were cultured in BEBM medium (Lonza, Walkersville, MD) with small airway epithelial cell growth factors kit. Medium was replaced with serum-free medium for 3 h prior to treatment.

Adenovirus infection

ATX cDNA with V5 tag at C-termini were inserted into Ad5 adenovirus vector with CMV promoter, its amplification and purification were services provided by Gene Transfer Vector Core, University of Iowa, Iowa. Equivalent titres of purified ATX adenovirus and empty control adenovirus (1-10 MOI) were added to cell culture (without FBS) for 24 or 48 h.

Preparation of LPA, LPC, and Brp-LPA

Lipids were prepared fresh in a serum free medium with 0.1 % BSA before experiments. Lipids were evaporated under nitrogen and appropriate volumes of serum free medium with 0.1% BSA were added to prepare 100 × stock solution. Lipids were resuspended by sonication.

Scratch Assay

Cells monolayer were scratched using a sterile 10 μl pipette tip. Nonadherent cells and cellular debris were removed by washing. After indicated time points, cells were digitally photographed and extent of cell migration was quantified using Image J software. The percentage of wound closure was calculated as follow: [(pre-migration area – migration area) / pre-migration area] × 100 [36]. All the scratch assay were performed in serum free medium.

Transwell invasion assay

Transwell invasion assay kit was purchased from Trevigen Inc. (Gaithersburgh, MD). Briefly, to determine the effect of released ATX-V5 on cell migration, 100 μl of A549 cells (1×10^5) in ATX-V5 overexpressed conditional medium or control conditional medium were added to top chamber and 500 μl of serum free RPMI-1640 medium were added to the bottom chamber. After 18 h incubation at 37 °C, media from the top and bottom chambers were aspirated. Cells migrated inside the chamber were dissociated with Cell Dissociation/ Calcein-AM and degree of cell invasion was examined by fluorescence microplate reader with 488 nm excitation and 520 nm emission. To determine the chemotaxis effect of ATX-V5, cells in serum free RPMI-1640 medium were added to the top chamber and ATX-V5 overexpressed conditional medium was added to the bottom chamber.

ATX activity assay

Fluorescence FS-3 was used as substrate to measure ATX activity. 10μl of conditional media were incubated with FS-3 (5 μM) in reaction buffer (50mM Tris pH8.0, 120 mM NaCl, 5 mM KCl, 1 mM CaCl2, 5 mM MgCl2) in a 96-well plate for indicated times. Results were determined by a microplate reader with 488 nm excitation and 520 nm emission.

Immunofluorescence microscopy

Cells were fixed in 3.7 % of formaldehyde for 20 min, followed by permealization with 0.1 % of Triton-100 for 2 min. Changes in ATX, p-PKCδ, p-cortactin, cortactin, and integrin β4 were examined by immunofluorescence staining by incubating with specific primary antibodies and fluorescence labeled secondary antibodies. Images were captured by Nikon ECLIPSE TE 300 inverted microscope.

Immunoprecipitation and Western blotting

Cell lysates were subjected to SDS-PAGE, electrotransfered to membranes and immunoblotted as described [18]. For immunoprecipitation, equal amounts of cell lysates (500 μg) were incubated with 2 μg/ml specific primary antibodies overnight at 4 °C followed by the addition of 40 μl of protein A/G-agarose followed for 2 h at 4°C. The immunoprecipitated complex was washed three times with ice-cold phosphate-buffered saline and analyzed by Western blotting with an enhanced ECL system.

RNA extraction and Real time RT-PCR

Total RNA from cells or lung tissues was extracted by TRIzol (Sigma) according to manufacturer's instructions. 1 μg of RNA was reverse transcribed using cDNA synthesis kit (Bio-Rad) and Real-time PCR was performed to assess expression of ATX mRNA as previously described [18]. Mouse ATX primers used were, mATX forward: GAAACAGCACCTTCCCAAAC, and mATX reverse: AAGGTTTCCTTGCAACATGC. Amplicon expression in each sample was normalized to its 18S RNA content. The relative abundance of target mRNA in each sample was calculated using the following formula: $\{2^{-(\text{ATX Threshold Cycle})}/2^{-(\text{18S Threshold Cycle})}\}\times 10^6$.

LPA measurement

LPA levels in the medium and BAL fluids were determined using liquid chromatography and tandem mass spectrometry (LC) with ABI-4000 Q-TRAP hybrid triple quadrupole/ion trap mass spectrometer (MS) coupled with an Agilent 1100 liquid chromatography system [30].

LPS-induced murine model of ALI

Sv/129 mice (Jackson Laboratory, Bar Harbor, ME) were housed in a specific pathogen-free barrier facility maintained by the University of Chicago Animal Resources Center. Adult male mice, 8–10-week old, with an average weight of 20–25 g were anaesthetized with a mixture of 25 mg/kg of ketamine and 2.5 ml of xylazine. LPS (5 mg/kg body weight) or water alone were intratracheally delivered. After 24 h, BAL fluids were collected by an intratracheal injection of 1 ml of PBS solution followed by gentle aspiration. The lavage was repeated twice to recover a total volume of 1.8-2.0 ml and LPA levels were measured by LC/MS/MS and ATX levels were determined by Western blotting. All animal experiments were approved by the University of Chicago Institutional Animal Care & Use Committee (Chicago, IL, USA) for the humane treatment of experimental animals and were performed at University of Chicago.

Statistics—All results were subjected to statistical analysis using one-way ANOVA and, wherever appropriate, analyzed by Student–Newman-Keuls test. Data are expressed as mean ± S.D. of triplicate samples from at least three independent experiments and values that were $P<0.5$ were considered statistically significant.

RESULTS

ATX is secreted from lung epithelial cells—Although overexpressed ATX is released from various cell types, the endogenous ATX secretion has not been well demonstrated. In order to address this question, we replaced lung epithelial cells (A549 cells) culture medium with serum-free medium for 1-6 h, and then collected the culture supernatant, concentrated, and determined the relative levels of secreted ATX by immunoblotting (Figure 1A). Furthermore, A549 cells were also infected with recombinant adenovirus capable of expressing ATX - V5 tag (10 MOI, 24 h and 48 h), and the ATX-V5 secreted into culture supernatant was also detected in the medium by antibodies against ATX as well as the V5 tag (Figure 1B). ATX activities in the same conditional medium were measured using FS-3 fluorescence. ATX activity significantly increased in ATX-V5 overexpressed (24 h and 48 h) cell culture supernatant (Figure 1C). Double immunostaining with antibodies to ATX and V5 revealed that over-expressed ATX was localized in perinuclear and exocytotic vesicle like bodies (Figure 1D).

ATX stimulates cell migration—To investigate the role of ATX in cell migration, ATX expression was down-regulated by transfection with ATX siRNA and the results are shown in Figure 2A. Transfection of cells with ATX siRNA but not control siRNA resulted in significant reduction in ATX protein (Figure 2A inset) and activity (Figure 2A). There was also significant reduction in cell migration at 24 and 48 h (Figure 2B). Further, pretreatment of A549 cells for 24 h with increasing concentrations of Brp-LPA, an inhibitor of ATX, attenuated cell migration at 24 and 48 h (Figure 2C). Overexpression of ATX-V5 by infection with ATX-V5 recombinant adenovirus enhanced cell migration (Figure 2D). These results demonstrated a role of ATX in lung epithelial cell migration.

Secreted ATX shows lysoPLD activity and induces cell migration via LPA generation and LPA_1 receptor—As ATX is known to regulate cell migration, we next investigated whether released ATX has lysoPLD activity. Serum free supernatant collected from A549 cells infected with ATX-V5 adenovirus (10 MOI, 24 h) was incubated with egg lysophosphatidylcholine (egg LPC, 0, 10, 50, 200 μM), and the LPA species in the culture supernatants were measured by LC/MS/MS. Egg LPC increases LPA generation in a dose dependent manner (Table 1). Total LPA levels increased ~27.3 fold in the presence of 200 μM of LPC (0 μM of LPC: 2.40 ± 0.55 vs. 200 μM of LPC: 862.30 ± 92.60 fmol/ml) indicating ability of endogenous secreted ATX to hydrolyze added egg LPC. 16:0 LPA is major product generated from egg LPC. Furthermore, heat-inactivated (60 °C for 30 min) ATX-V5 overexpressed conditional medium was had no ability to increase LPA levels in presence of egg LPC.

We next determined the effects of control medium and ATX-V5 overexpressed (1, 5, and 10 MOI, 24 h) conditional medium on cell migration by scratch (Fig. 3A) and transwell assays (Fig. 3B). ATX-V5 overexpressed medium induced significant cell migration compared to cells exposed to control medium from empty adenovirus vector-infected cells. In transwell assay, addition of the ATX-V5 overexpressed conditional medium to bottom chamber had no effect on cell invasion (data not shown), suggesting that ATX-V5 induces cell motility, and not chemotaxis. We further substantiated the above results using human small airway epithelial cells (Fig. 3B). Furthermore, we investigated effect of the addition of LPC (0 – 200 μM) on ATX-V5 overexpressed medium-induced cell migration. LPC alone, at all the concentrations tested, had no effect on cell migration, while 10 and 50 μM of LPC enhanced ATX-V5 overexpressed (10 MOI, 24 h) conditional medium-induced cell migration as determined by scratch (Fig. 3C) and transwell assays (Fig. 3D). Though higher concentration of LPC (100 and 200 μM) generated much higher levels of LPA, however, the relatively higher LPA levels did not promote ATX-V5 medium-induced migration..

Incubation with an antibody to V5 attenuated ATX-V5 medium-mediated migration (Fig. 3E). Immunofluoescence microscopy study showed that ATX-V5 medium induced actin rearrangement (Fig. 3F).

To investigate whether ATX-V5 overexpressed conditional medium-induced cell migration through LPA generation and ligation to the LPA receptors, pre-treatment of cells with the $LPA_{1\&3}$ antagonist, ki16425 (10 μM), partially blocked ATX-V5-induced cell migration. The inhibition was much greater with respect to LPA-induced migration (Fig. 4A). As expected, downregulation of LPA_1 by LPA_1 siRNA (50 nM, 72 h) (Figure 4B) or pretreatment with pertussis toxin (100 ng/ml, 4 h) (Figure 4C) attenuated both ATX-V5 and LPA-mediated cell migration. These results demonstrate that the medium from ATX-V5 over-expressing cells is biologically active and sufficient to stimulate LPA generation and cell migration via $G_{\alpha i}$-coupled LPA_1.

PKCδ regulates ATX-induced cell migration—We have previously shown that LPA activates PKCδ and this contributes to LPA-mediated signaling, such as IL-8 secretion and EGF-R transactivation in human bronchial epithelial cells [18, 37-39]. As ATX induces LPA generation and stimulates cell migration, we investigated the role of PKCδ on ATX-V5-mediated cell migration. Treatment of A549 cells with ATX-V5 medium or LPA (1 μM) for 3 h increased phosphorylation of PKCδ in leading edges of the cell as evidenced by immunostaining with an antibody to phospho-PKCδ (Fig. 5A). Overexpression of dominant-negative (dn) PKCδ by adenoviral infection (10 MOI) for 24h significantly attenuated ATX-V5 medium-mediated cell migration (vector control: 46.5 ± 6.2%; dn-PKCδ: 23.1 ± 12.1%); however, overexpression of dn-PKCζ (10 MOI, 24 h) and dn-PKCα (10 MOI, 24 h) had no effect on ATX-V5 overexpressed conditional medium-mediated migration (Fig. 5B), suggesting PKCδ, but not other PKC isoforms regulate ATX-V5-mediated cell migration.

Involvement of cortactin in ATX-mediated cell migration—Cortactin, an actin binding protein, is also known to play a positive role in cell migration through cytoskeletal rearrangement [11, 13, 40]. To investigate the role of cortactin in ATX mediated cell migration, A549 cells were exposed to ATX-V5 medium or LPA (1 μM) for 3 h. As shown in Fig. 6A, ATX-V5 medium induced phosphorylation of cortactin in leading edge of migrating cells. Further, Western blotting showed that ATX-V5 medium or LPA increased tyrosine phosphorylation of cortactin in A549 cells (Fig. 6B). Overexpression of dn-PKCδ (10 MOI, 24 h) attenuated ATX-V5 medium or LPA-induced phosphorylation of cortactin (Fig. 6A, B). To further investigate the role of cortactin in ATX-V5 medium-induced cell migration, cortactin expression was downregulated by transfection of cells with cortactin specific siRNA (50 nM, 72 h). As shown in Fig. 6C, cells transduced with cortactin siRNA demonstrated significantly attenuated ATX-V5 medium- or LPA-enhanced cell migration. The effect of cortactin siRNA on cortactin protein expression was confirmed by Western blotting (Fig. 6D). These results suggested that ATX-V5 dependent tyrosine phosphorylation of cortactin is mediated by PKCδ, and underscored the role of cortactin in ATX-V5-mediated cell migration.

Extracellular ATX-V5 interacts with LPA_1 and integrin β4—To investigate the lysoPLD activity dependence of the effect of secreted ATX on migration, cells were treated with recombinant wild type ATX (rATX Wt) or a catalytically inactive ATX mutant (rATX Mt T210A) protein (100 ng/ml). As shown in Fig. 7A, both ATX wild type and the inactive mutant enhanced A549 and HSAEpCs cell migration; however, rATX Wt increased cell migration to a greater extent compared to mutant rATX. Both rATX Wt and rATX Mt increased phosphorylation of cortactin (Figure 7B). Further, heat inactivated ATX-V5 conditional medium revealed loss of ATX activity as revealed by LC/MS/MS (Table 1) and by using FS-3 as substrate (Figure 7C). Cells exposed to ATX-V5 conditional medium and

heat-inactivated ATX-V5 conditional medium enhanced migration, compare to cells exposed control conditional medium (Figure 7D). Addition of LPC (50 μM) further enhanced ATX-V5 conditional medium-induced cell migration, while it had no effect on heat-inactivated ATX-V5 medium-induced migration. These results suggest that extracellular ATX-induced cell migration was not totally dependent on ATX catalytic activity and LPA generation.

ATX has been shown to bind to the cell surface via integrin β in activated lymphocytes [41] and platelets [34]. To determine whether extracellular ATX binds to the lung epithelial cell surface receptors, A549 cells were treated with ATX-V5 medium for 15 -120 min, cells were washed stringently several times and cell lysates were prepared. As shown in Fig. 7E, secreted ATX-V5 was detected in cell lysates after ATX-V5 medium treatment, which suggests that secreted ATX-V5 bound to the cell surface. To investigate whether ATX-V5 binds to LPA receptors or other migration-related proteins on cell surface, cells were exposed to ATX-V5 conditional medium or heated inactivated ATX-V5 conditional medium for 1 h, ATX-V5 or LPA_1 was immunoprecipitated and processed for immunoblotting. The data revealed that both of ATX-V5 and heat inactivated ATX-V5 associated with LPA_1 and integrin β4 (Fig. 7F and 7G). Immunostaining with antibodies to ATX and integrin β4 showed that ATX-V5 conditional medium induced integrin β4 accumulation at the leading edge and significantly co-localized with ATX-V5 (Figure 7H). These results indicated that interaction of released ATX with LPA_1 and integrin β4 may contribute to extracellular ATX-mediated cell migration.

LPS challenge induces ATX expression and release into BAL fluid—ATX is present in plasma and serum and alterations in ATX levels have been detected in various disorders [42-44]. We therefore measured ATX levels in BAL fluid in a murine model of LPS-induced acute lung injury. Hematoxylin and Eosin (H&E) staining of lung tissue after intratracheal administration of LPS (5 mg/kg body weight, 24 h) showed a significant increase in infiltration of inflammatory cells into the alveolar space (Fig. 8A). Analysis of ATX mRNA levels in lung tissue of LPS (1 and 5 mg/kg body weight, 24 h) challenged mice by real time RT-PCR showed increased mRNA expression of ATX compared to control mice (Figs. 8B). Analysis of ATX levels in BAL fluids by Western blotting showed that LPS challenge increased ATX secretion in BAL fluids, compared to control mice (Fig. 8C). Furthermore, LPA levels in BAL fluids (control: 47.0 +4.0; LPS: 110.3 + 32.5 fmol/ml) were increased in LPS challenged mice. Among the LPA species, the levels of 16:1LPA, 16:0LPA, 18:2LPA, 18:1LPA, 20:4LPA, and 20:3LPA significantly increased (~1.5-10.2 fold) in LPS-challenged BAL fluids (Fig. 8D).

DISCUSSION

Originally identified as a tumor cell autocrine motility factor, ATX plays a major role in extracellular LPA generation through its intrinsic lysoPLD activity [25]. ATX induces cell motility by producing LPA which acts on LPA receptors [21, 22, 25, 34]; however, the molecular signaling pathway downstream of ATX/LPA/LPA-R, which triggers cell migration has not been well characterized. The present study provides the first evidence that secreted ATX induced cell migration through the LPA/LPA_1 signaling axis involving a Ca^{2+}-insensitive PKC isoform, PKCδ, and cortactin, both present in the leading edges of migrating cells. Another novel observation here is that extracellular ATX induced cell migration partially through a LPA generation-independent pathway. Our results suggested that extracellular ATX interacted with the LPA receptor and integrin β4 on the epithelial cell surface to elicit lung epithelia cell motility (Figure 9). The data presented here also raise the possibility that PKCδ might serve as a potential therapeutic target in lung injury.

LPA, the simplest lysophospholipid, is a growth factor that induces cell proliferation and migration [22, 25, 49]. Biological effects of LPA are mediated via ligation to G protein-coupled LPA receptors (LPA_{1-7}) expressed on cell surface [31, 32, 50, 51]. ATX is a key enzyme that regulates LPA levels in biological fluids such as plasma [34, 41, 52]. Plasma ATX levels have been known to increase in several disorders such as chronic hepatitis C [42], follicular lymphoma [43], and prostate cancer [44]. ATX is an autocrine protein; however, there is limited information on the release of ATX, its biological effects, and signaling in the context of epithelia. Here we found that endogenous ATX was secreted from alveolar epithelial cells *in vitro* and also *in vivo*, as observed in lung fluid of a murine model of acute lung injury. Secreted ATX increased lung epithelial cell migration through LPA generation and signaling via LPA_1 by phosphorylation of PKCδ and cortactin. Here, we show that adding 50 μM of egg LPC enhanced ATX-V5 conditional medium-mediated migration at maximal level, while 200 μM of egg LPC had no significant effect. This may due to some unknown side effects of higher concentration of egg LPC.

The current study underscored a potential fundamental role for PKCδ in cell motility. Our previous studies have demonstrated that PKCδ is a downstream target of LPA receptor signaling and regulates LPA-induced EGF-R transactivation [18], NF-κB activation [37], IL-8 secretion [18, 37], and E-cadherin / c-Met complex accumulation at cell-cell contacts [38, 39] in human lung epithelial cells. In dermal fibroblasts, PDGF-BB induces PKCδ accumulation at the migrating leading edge of cells and over-expression of dn-PKCδ blocks PDGF-BB-induced activation of signal transducer and activator of transcription 3 (Stat3) and cell migration [53]. Overexpression of PKCδ promotes Madin-Darby canine kidney cell membrane protrusions, cell spreading, and cell migration [54]. The current study further demonstrated that phosphorylation of PKCδ is mediated by extracellular ATX or LPA clusters at the leading edge and regulates extracellular ATX-induced cell migration. Interestingly, we also found that PKCζ and PKCα are not involved in extracelluar ATX-induced cell migration, though PKCζ has been known to regulate lung endothelial cell migration [36]. Our unpublished data shows that at least in lung epithelial cells, LPA has no ability to activate PKCα. Cortactin, an actin-associated scaffolding protein, is known to mediate cell migration [13, 40, 55]; and phosphorylation of cortactin by Src kinase enhances cortactin-mediated actin assembly [11, 13, 55]. In lung epithelial cells, LPA, the product of ATX induces phosphorylation of Src kinase [18]. A recent study suggests potential interaction between PKCδ and cortactin that in turn regulates PKCδ-mediated polymerization of actin [20]. These data suggest a role for PKCδ in activation and re-organization of cortactin. The results presented here demonstrated a role for PKCδ in ATX- and LPA-induced phosphorylation of cortactin in lung epithelial cells. The mechanism by which PKCδ, a serine/threonine kinase, regulates tyrosine phosphorylation of cortactin is unclear. PKCδ itself is unlikely to directly phosphorylate cortactin; however, interaction of PKCδ with cortactin is known to induce serine phosphorylation and activation of Src kinase in RBL-2H3 mast cell line [16] that may then target cortactin. We have previously shown that inhibition of PKCδ attenuated LPA-induced phosphorylation of Lyn kinase, a member of Src kinase family [18]. Taken together, these results indicated a role for PKCδ in cortactin phosphorylation, most likely through activation of a Src kinase.

Here, we show that ATX mutant and heat-inactivated ATX-V5 conditional medium induced cell migration, through their effects were less than wild type ATX and ATX-V5 conditional medium. Adding LPC enhanced ATX-V5 conditional medium-induced cell migration, while LPC had no effect on heat-inactivated ATX-V5 medium-mediated cell migration. These results suggested that exogenous ATX-induced migration is partly independent on lysoPLD activity. The carboxyl-terminus of ATX contains a Modulator of Oligodendrocyte Remodeling and Focal adhesion Organization (MORFO) domain, which potentiates binding to cell surface receptors and adhesion proteins [56, 57]. ATX also possesses an arginine-

glycine-aspartic acid (RGD) motif, which is a potential site for binding to integrins and it has been recently demonstrated that ATX binding to activated human platelets was inhibited by antibody to integrin β3 [34]. ATX binds to lymphocytes in an integrin β1-dependent manner [41], indicating a role for integrin in the regulation of extracellular ATX binding to cell surface. The current study showed that ATX mutant (T210A) also increased cell migration, though less effectively compared to the ATX wild type, suggesting that other pathway(s) independent of LPA generation are likely tomediate ATX mediated cell migration. Furthermore, we provide here evidence in support of extracellular ATX binding to lung epithelial cells. Interactions between G protein-coupled receptors and integrins have been reported. P2Y2 nucleotide receptor interacts with integrin αV in human 1321N1 astrocytoma cells [58, 59]. Recently, it was demonstrated that G protein subunit Gα13 binds to integrin αIIbβ3 [60]. Our results also indicated that ATX binds to a complex of cell surface proteins, including LPA_1 and integrin β4, leading to the supposition that ATX-induced cell migration may be through a more intricate mechanism involving domain-specific interactions with a complex of signaling molecules at the cell surface that transduces signals initiating cellular migration. Our future studies will focus on investigating the LPA receptor docking sites and binding domains of ATX.

Acknowledgments

The work was supported by National Institute of Health grant HL0911916 (to YZ), and HL 079396 (to VN), and University of Pittsburgh Medical Center Start Up fund (to YZ).

The abbreviations used are

ATX	autotaxin
LysoPLD	lysophospholipase D
LPA	lysophosphatidic acid
LPS	lipopolysaccharide
BAL	bronchoalveolar lavage

REFERENCES

1. Koizumi A, Sageshima M, Wada Y, Narita S, Higuchi S. Immature alveolar/blood barrier and low disaturated phosphatidylcholine in fetal lung after intrauterine exposure to O,O,S-trimethylphosphorothioate. Arch. Toxicol. 1989; 63:331–335. [PubMed: 2764722]
2. Sacco O, Silvestri M, Sabatini F, Sale R, Defilippi AC, Rossi GA. Epithelial cells and fibroblasts: structural repair and remodelling in the airways. Paediatr. Respir. Rev. 2004; 5(Suppl A):S35–40. [PubMed: 14980241]
3. Schneeberger EE, Karnovsky MJ. Substructure of intercellular junctions in freeze-fractured alveolar-capillary membranes of mouse lung. Circ. Res. 1976; 38:404–411. [PubMed: 1269080]
4. Corvol H, Flamein F, Epaud R, Clement A, Guillot L. Lung alveolar epithelium and interstitial lung disease. Int. J. Biochem. Cell. Biol. 2009; 41:1643–1651. [PubMed: 19433305]
5. Freeman BA, Panus PC, Matalon S, Buckley BJ, Baker RR. Oxidant injury to the alveolar epithelium: biochemical and pharmacologic studies. Research report (Health Effects Institute). 1993:1–30. discussion 31-39. [PubMed: 8439407]
6. Sugahara K, Tokumine J, Teruya K, Oshiro T. Alveolar epithelial cells: differentiation and lung injury. Respirology. 2006; 11(Suppl):S28–31. [PubMed: 16423267]
7. Koff JL, Shao MX, Kim S, Ueki IF, Nadel JA. Pseudomonas lipopolysaccharide accelerates wound repair via activation of a novel epithelial cell signaling cascade. J. Immunol. 2006; 177:8693–8700. [PubMed: 17142770]

8. Atkinson JJ, Adair-Kirk TL, Kelley DG, Demello D, Senior RM. Clara cell adhesion and migration to extracellular matrix. Respir. res. 2008; 9:1. [PubMed: 18179694]
9. Desai LP, Chapman KE, Waters CM. Mechanical stretch decreases migration of alveolar epithelial cells through mechanisms involving Rac1 and Tiam1. Am J Physiol Lung Cell Mol. Physiol. 2008; 295:L958–965. [PubMed: 18805958]
10. Lesur O, Arsalane K, Lane D. Lung alveolar epithelial cell migration in vitro: modulators and regulation processes. Am. J. Physiol. 1996; 270:L311–319. [PubMed: 8638722]
11. Huang C, Liu J, Haudenschild CC, Zhan X. The role of tyrosine phosphorylation of cortactin in the locomotion of endothelial cells. J. Biol. Chem. 1998; 273:25770–25776. [PubMed: 9748248]
12. Kruchten AE, Krueger EW, Wang Y, McNiven MA. Distinct phospho-forms of cortactin differentially regulate actin polymerization and focal adhesions. Am. J. Physiol. 2008; 295:C1113–1122.
13. Lua BL, Low BC. Cortactin phosphorylation as a switch for actin cytoskeletal network and cell dynamics control. FEBS letters. 2005; 579:577–585. [PubMed: 15670811]
14. Durieu-Trautmann O, Chaverot N, Cazaubon S, Strosberg AD, Couraud PO. Intercellular adhesion molecule 1 activation induces tyrosine phosphorylation of the cytoskeleton-associated protein cortactin in brain microvessel endothelial cells. J. Biol. Chem. 1994; 269:12536–12540. [PubMed: 7909803]
15. Brandt DT, Goerke A, Heuer M, Gimona M, Leitges M, Kremmer E, Lammers R, Haller H, Mischak H. Protein kinase C delta induces Src kinase activity via activation of the protein tyrosine phosphatase PTP alpha. J. Biol. Chem. 2003; 278:34073–34078. [PubMed: 12826681]
16. Song JS, Swann PG, Szallasi Z, Blank U, Blumberg PM, Rivera J. Tyrosine phosphorylation-dependent and -independent associations of protein kinase C-delta with Src family kinases in the RBL-2H3 mast cell line: regulation of Src family kinase activity by protein kinase C-delta. Oncogene. 1998; 16:3357–3368. [PubMed: 9692543]
17. Pula G, Crosby D, Baker J, Poole AW. Functional interaction of protein kinase Calpha with the tyrosine kinases Syk and Src in human platelets. J. Biol. Chem. 2005; 280:7194–7205. [PubMed: 15583006]
18. Zhao Y, He D, Saatian B, Watkins T, Spannhake EW, Pyne NJ, Natarajan V. Regulation of lysophosphatidic acid-induced epidermal growth factor receptor transactivation and interleukin-8 secretion in human bronchial epithelial cells by protein kinase Cdelta, Lyn kinase, and matrix metalloproteinases. J. Biol. Chem. 2006; 281:19501–19511. [PubMed: 16687414]
19. Kiley SC, Clark KJ, Goodnough M, Welch DR, Jaken S. Protein kinase C delta involvement in mammary tumor cell metastasis. Cancer Res. 1999; 59:3230–3238. [PubMed: 10397270]
20. Llado A, Timpson P, Vila de Muga S, Moreto J, Pol A, Grewal T, Daly RJ, Enrich C, Tebar F. Protein kinase Cdelta and calmodulin regulate epidermal growth factor receptor recycling from early endosomes through Arp2/3 complex and cortactin. Mol. Biol. Cell. 2008; 19:17–29. [PubMed: 17959830]
21. Gaetano CG, Samadi N, Tomsig JL, Macdonald TL, Lynch KR, Brindley DN. Inhibition of autotaxin production or activity blocks lysophosphatidylcholine-induced migration of human breast cancer and melanoma cells. Mol. Carcinogen. 2009; 48:801–809.
22. Khurana S, Tomar A, George SP, Wang Y, Siddiqui MR, Guo H, Tigyi G, Mathew S. Autotaxin and lysophosphatidic acid stimulate intestinal cell motility by redistribution of the actin modifying protein villin to the developing lamellipodia. Exp. Cell. Res. 2008; 314:530–542. [PubMed: 18054784]
23. Stracke ML, Krutzsch HC, Unsworth EJ, Arestad A, Cioce V, Schiffmann E, Liotta LA. Identification, purification, and partial sequence analysis of autotaxin, a novel motility-stimulating protein. J. Biol. Chem. 1992; 267:2524–2529. [PubMed: 1733949]
24. Xu X, Prestwich GD. Inhibition of tumor growth and angiogenesis by a lysophosphatidic acid antagonist in an engineered three-dimensional lung cancer xenograft model. Cancer. 2010; 116:1739–1750. [PubMed: 20143443]
25. Umezu-Goto M, Kishi Y, Taira A, Hama K, Dohmae N, Takio K, Yamori T, Mills GB, Inoue K, Aoki J, Arai H. Autotaxin has lysophospholipase D activity leading to tumor cell growth and

motility by lysophosphatidic acid production. J. Cell. Biol. 2002; 158:227–233. [PubMed: 12119361]

26. van Meeteren LA, Moolenaar WH. Regulation and biological activities of the autotaxin-LPA axis. Prog. Lipid Res. 2007; 46:145–160. [PubMed: 17459484]
27. Nakanaga K, Hama K, Aoki J. Autotaxin - an LPA producing enzyme with diverse functions. J. Biochem. 2010; 148:13–24. [PubMed: 20495010]
28. Xu Y, Shen Z, Wiper DW, Wu M, Morton RE, Elson P, Kennedy AW, Belinson J, Markman M, Casey G. Lysophosphatidic acid as a potential biomarker for ovarian and other gynecologic cancers. Jama. 1998; 280:719–723. [PubMed: 9728644]
29. Sugiura T, Nakane S, Kishimoto S, Waku K, Yoshioka Y, Tokumura A. Lysophosphatidic acid, a growth factor-like lipid, in the saliva. J. Lipid Res. 2002; 43:2049–2055. [PubMed: 12454265]
30. Georas SN, Berdyshev E, Hubbard W, Gorshkova IA, Usatyuk PV, Saatian B, Myers AC, Williams MA, Xiao HQ, Liu M, Natarajan V. Lysophosphatidic acid is detectable in human bronchoalveolar lavage fluids at baseline and increased after segmental allergen challenge. Clin. Exp. Allergy. 2007; 37:311–322. [PubMed: 17359381]
31. Zhao Y, Natarajan V. Lysophosphatidic acid signaling in airway epithelium: role in airway inflammation and remodeling. Cell. Signal. 2009; 21:367–377. [PubMed: 18996473]
32. Anliker B, Chun J. Cell surface receptors in lysophospholipid signaling. Semin. Cell. Dev. Biol. 2004; 15:457–465. [PubMed: 15271291]
33. Ye X, Ishii I, Kingsbury MA, Chun J. Lysophosphatidic acid as a novel cell survival/apoptotic factor. Biochim. Biophys. Acta. 2002; 1585:108–113. [PubMed: 12531543]
34. Pamuklar Z, Federico L, Liu S, Umezu-Goto M, Dong A, Panchatcharam M, Fulerson Z, Berdyshev E, Natarajan V, Fang X, van Meeteren LA, Moolenaar WH, Mills GB, Morris AJ, Smyth SS. Autotaxin/lysopholipase D and lysophosphatidic acid regulate murine hemostasis and thrombosis. J. Biol. Chem. 2009; 284:7385–7394. [PubMed: 19139100]
35. Yang Y, Mou L, Liu N, Tsao MS. Autotaxin expression in non-small-cell lung cancer. Am. J. Respir. Cell. Mol. Biol. 1999; 21:216–222. [PubMed: 10423404]
36. Gorshkova I, He D, Berdyshev E, Usatuyk P, Burns M, Kalari S, Zhao Y, Pendyala S, Garcia JG, Pyne NJ, Brindley DN, Natarajan V. Protein kinase C-epsilon regulates sphingosine 1-phosphate-mediated migration of human lung endothelial cells through activation of phospholipase D2, protein kinase C-zeta, and Rac1. J. Biol. Chem. 2008; 283:11794–11806. [PubMed: 18296444]
37. Cummings R, Zhao Y, Jacoby D, Spannhake EW, Ohba M, Garcia JG, Watkins T, He D, Saatian B, Natarajan V. Protein kinase Cdelta mediates lysophosphatidic acid-induced NF-kappaB activation and interleukin-8 secretion in human bronchial epithelial cells. J. Biol. Chem. 2004; 279:41085–41094. [PubMed: 15280372]
38. He D, Su Y, Usatyuk PV, Spannhake EW, Kogut P, Solway J, Natarajan V, Zhao Y. Lysophosphatidic acid enhances pulmonary epithelial barrier integrity and protects endotoxin-induced epithelial barrier disruption and lung injury. J. Biol. Chem. 2009; 284:24123–24132. [PubMed: 19586906]
39. Zhao Y, He D, Stern R, Usatyuk PV, Spannhake EW, Salgia R, Natarajan V. Lysophosphatidic acid modulates c-Met redistribution and hepatocyte growth factor/c-Met signaling in human bronchial epithelial cells through PKC delta and E-cadherin. Cell. Signal. 2007; 19:2329–2338. [PubMed: 17689924]
40. Buday L, Downward J. Roles of cortactin in tumor pathogenesis. Biochim. Biophys. Acta. 2007; 1775:263–273. [PubMed: 17292556]
41. Kanda H, Newton R, Klein R, Morita Y, Gunn MD, Rosen SD. Autotaxin, an ectoenzyme that produces lysophosphatidic acid, promotes the entry of lymphocytes into secondary lymphoid organs. Nature Immunol. 2008; 9:415–423. [PubMed: 18327261]
42. Watanabe N, Ikeda H, Nakamura K, Ohkawa R, Kume Y, Aoki J, Hama K, Okudaira S, Tanaka M, Tomiya T, Yanase M, Tejima K, Nishikawa T, Arai M, Arai H, Omata M, Fujiwara K, Yatomi Y. Both plasma lysophosphatidic acid and serum autotaxin levels are increased in chronic hepatitis C. J. Clin. Gastroenterol. 2007; 41:616–623. [PubMed: 17577119]
43. Masuda A, Nakamura K, Izutsu K, Igarashi K, Ohkawa R, Jona M, Higashi K, Yokota H, Okudaira S, Kishimoto T, Watanabe T, Koike Y, Ikeda H, Kozai Y, Kurokawa M, Aoki J, Yatomi Y. Serum

autotaxin measurement in haematological malignancies: a promising marker for follicular lymphoma. Brit. J. Haematol. 2008; 143:60–70. [PubMed: 18710386]

44. Nakamura K, Takeuchi T, Ohkawa R, Okubo S, Yokota H, Tozuka M, Aoki J, Arai H, Ikeda H, Ohshima N, Kitamura T, Yatomi Y. Serum lysophospholipase D/autotaxin may be a new nutritional assessment marker: study on prostate cancer patients. Ann. Clin. Biochem. 2007; 44:549–556. [PubMed: 17961310]
45. Hayakawa J, Okabayashi Y. Simultaneous analysis of phospholipid in rabbit bronchoalveolar lavage fluid by liquid chromatography/mass spectrometry. J. Pharm. Biomed. Anal. 2004; 35:583–592. [PubMed: 15137983]
46. Barroso B, Bischoff R. LC-MS analysis of phospholipids and lysophospholipids in human bronchoalveolar lavage fluid. J. Chromatogr. 2005; 814:21–28.
47. Arbibe L, Koumanov K, Vial D, Rougeot C, Faure G, Havet N, Longacre S, Vargaftig BB, Bereziat G, Voelker DR, Wolf C, Touqui L. Generation of lyso-phospholipids from surfactant in acute lung injury is mediated by type-II phospholipase A2 and inhibited by a direct surfactant protein A-phospholipase A2 protein interaction. J. Clin. Invest. 1998; 102:1152–1160. [PubMed: 9739049]
48. Kennedy M, Phelps D, Ingenito E. Mechanisms of surfactant dysfunction in early acute lung injury. Exp. Lung Res. 1997; 23:171–189. [PubMed: 9184787]
49. van Leeuwen FN, Giepmans BN, van Meeteren LA, Moolenaar WH. Lysophosphatidic acid: mitogen and motility factor. Biochem. Soc. Trans. 2003; 31:1209–1212. [PubMed: 14641027]
50. Chun J. Lysophospholipid receptors: implications for neural signaling. Crit. Rev. Neurobiol. 1999; 13:151–168. [PubMed: 10512488]
51. Radeff-Huang J, Seasholtz TM, Matteo RG, Brown JH. G protein mediated signaling pathways in lysophospholipid induced cell proliferation and survival. J. Biol. Chem. 2004; 92:949–966.
52. Ferry G, Giganti A, Coge F, Bertaux F, Thiam K, Boutin JA. Functional invalidation of the autotaxin gene by a single amino acid mutation in mouse is lethal. FEBS letters. 2007; 581:3572–3578. [PubMed: 17628547]
53. Fan J, Guan S, Cheng CF, Cho M, Fields JW, Chen M, Denning MF, Woodley DT, Li W. PKCdelta clustering at the leading edge and mediating growth factor-enhanced, but not ecm-initiated, dermal fibroblast migration. J. Invest. Dermatol. 2006; 126:1233–1243. [PubMed: 16543902]
54. Chen CL, Hsieh YT, Chen HC. Phosphorylation of adducin by protein kinase Cdelta promotes cell motility. J. Cell Sci. 2007; 120:1157–1167. [PubMed: 17341583]
55. Ren G, Crampton MS, Yap AS. Cortactin: Coordinating adhesion and the actin cytoskeleton at cellular protrusions. Cell. Mot. Cytosk. 2009; 66:865–873.
56. Dennis J, White MA, Forrest AD, Yuelling LM, Nogaroli L, Afshari FS, Fox MA, Fuss B. Phosphodiesterase-Ialpha/autotaxin's MORFO domain regulates oligodendroglial process network formation and focal adhesion organization. Mol. Cell. Neurosci. 2008; 37:412–424. [PubMed: 18164210]
57. Yuelling LM, Fuss B. Autotaxin (ATX): a multi-functional and multi-modular protein possessing enzymatic lysoPLD activity and matricellular properties. Biochim Biophys Acta. 2008; 1781:525–530. [PubMed: 18485925]
58. Liao Z, Seye CI, Weisman GA, Erb L. The P2Y2 nucleotide receptor requires interaction with alpha v integrins to access and activate G12. Journal of cell science. 2007; 120:1654–1662. [PubMed: 17452627]
59. Wang M, Kong Q, Gonzalez FA, Sun G, Erb L, Seye C, Weisman GA. P2Y nucleotide receptor interaction with alpha integrin mediates astrocyte migration. J Neurochem. 2005; 95:630–640. [PubMed: 16135088]
60. Gong H, Shen B, Flevaris P, Chow C, Lam SC, Voyno-Yasenetskaya TA, Kozasa T, Du X. G protein subunit Galpha13 binds to integrin alphaIIbbeta3 and mediates integrin "outside-in" signaling. Science. 2010; 327:340–343. [PubMed: 20075254]

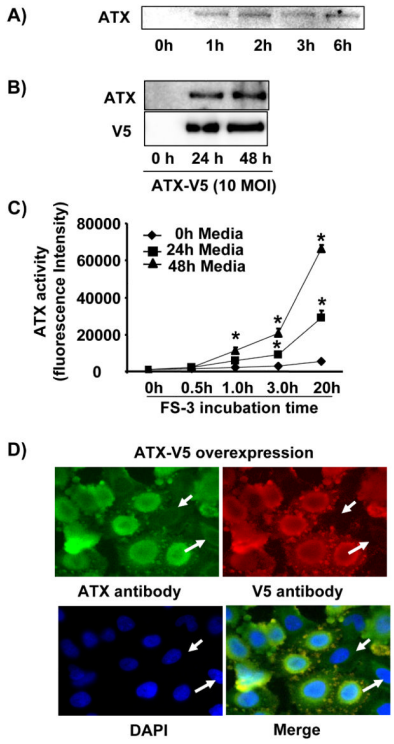

Figure 1. A549 cells release ATX

A) Serum free-culture medium was collected after incubation of cells for 1-6 h, and the presence of ATX was determined by immunoblotting with an anti-ATX antibody. Shown is a representative blot from three independent experiments. B) A549 cells were infected with ATX-V5 adenovirus (10 MOI) for 24 h and 48 h. ATX-V5 present in culture supernatant was determined by imunoblotting using antibodies against ATX and V5. Shown are representative blots from three independent experiments. C) Conditional medium from above was incubated with FS-3 for indicated times (0 - 20 h) and fluorescence was measured. The graph represents ATX activity (mean ± S.D.) from three independent experiments. *$p<0.01$, compared to control medium. D) Cells were infected with ATX-V5 (10 MOI, 24 h), and immunostained with antibodies against ATX and V5 tag. Shown are representative images from three independent experiments.

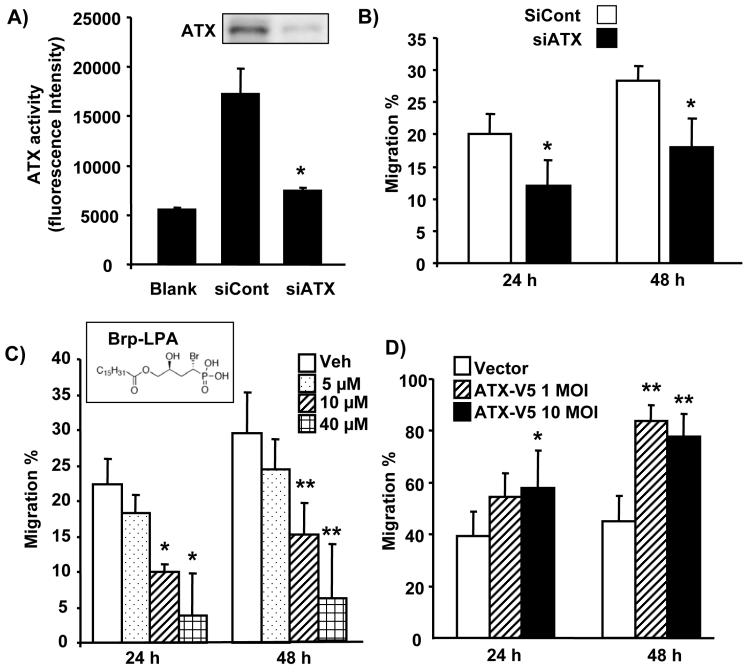

Figure 2. ATX regulates cell migration

A) A549 cells were transfected with scrambled or ATX siRNA (50 nM) for 48 h. Cell culture media were replaced with serum-free medium and after 24 h, serum free culture supernatants collected and concentrated. ATX activities were measured with fluorescence microreader after incubation with FS-3 for 20 h. The data represents mean ± S.D. from three independent experiments. *$p<0.01$, compared to scrambled siRNA transfected groups. Insert shows the presence of ATX in medium as detected by Western blotting with antibody to ATX. B) A549 cell migration was measured by a scratch assay for 24 h in serum free medium. The data represent mean ± S.D. from three independent experiments. *$p<0.05$, compared to scrambled siRNA transduced cells. C) A549 cells were incubated with the ATX inhibitor, Brp-LPA, for 24 h and 48 h in serum free medium, and cell migration was measured by the scratch assay. The data represents mean ± S.D. from three independent experiments *$p<0.05$, compared to control cells at 24 h; and ** the same at 48 h. Brp-LPA molecular structure is shown in insert. D) A549 cells were infected with ATX-V5 adenovirus (10 MOI) for 24 h and 48 h, and then cell migration in serum free medium was measured by the scratch assay. The data represents mean ± S.D. from three independent experiments. * represents statistical significance ($p<0.05$) between ATX-V5 overexpressing cells and their control counterparts at 24 h; and ** the same at 48 h.

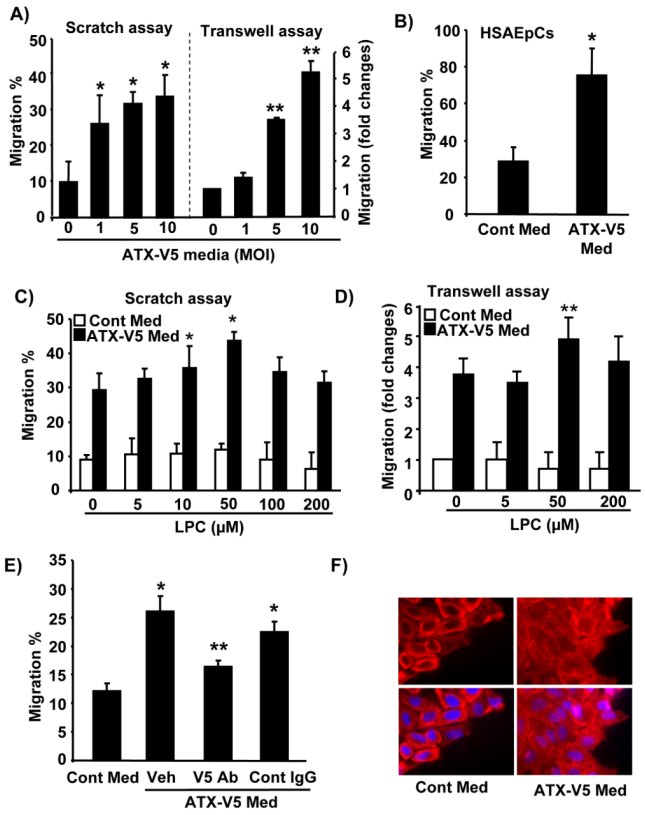

Figure 3. ATX-V5 increases LPA levels and cell migration

A) A549 cells were incubated with serum free medium from empty virus infected A549 cells (Cont Med) or from adenovirus encoding ATX-V5 (1-10 MOI, 24 h) infected A549 cells (ATX-V5 Med) and cell migration was measured at 18 h by scratch and transwell migration assay. The data represents mean ± S.D. from three independent experiments. *p<0.05, compared to vector control medium in scratch assay; *p<0.01, compared to vector control medium in transwell assay B) HSAEpCs were incubated with serum free Cont Med or ATX-V5 Med for 18 h, and cell migration was measured by scratch assay at 18 h. The data represents mean ± S.D. from three independent experiments. *p<0.01, compared to vector control medium. C) A549 cells were incubated with serum free Cont Med or ATX-V5 Med with or without egg LPC (0 – 200 μM), and cell migration was measured at 18 h by scratch assay and transwell migration assay (D). The data represents mean ± S.D. from three independent experiments. *p<0.05, compared to control medium in scratch assay; *p<0.05, compared to control medium in transwell assay. E) ATX-V5 Med was incubated with an antibody to V5 tag or IgG control (10 μg/ml) overnight, and then was added to scratched cells. After 18 h, migration was measured. The data represents mean ± S.D. from three independent experiments. *p<0.05, compared to Cont Med-treated cells; **p<0.05, compared to ATX-V5 Med alone or plus control IgG-treated cells. F) A549 cells were treated with Cont Med or ATX-V5 Med for 18 h and actin microfilaments were immunostained by Texas Red-labeled phalloidin for 1 h. Shown are representative images from three independent experiments.

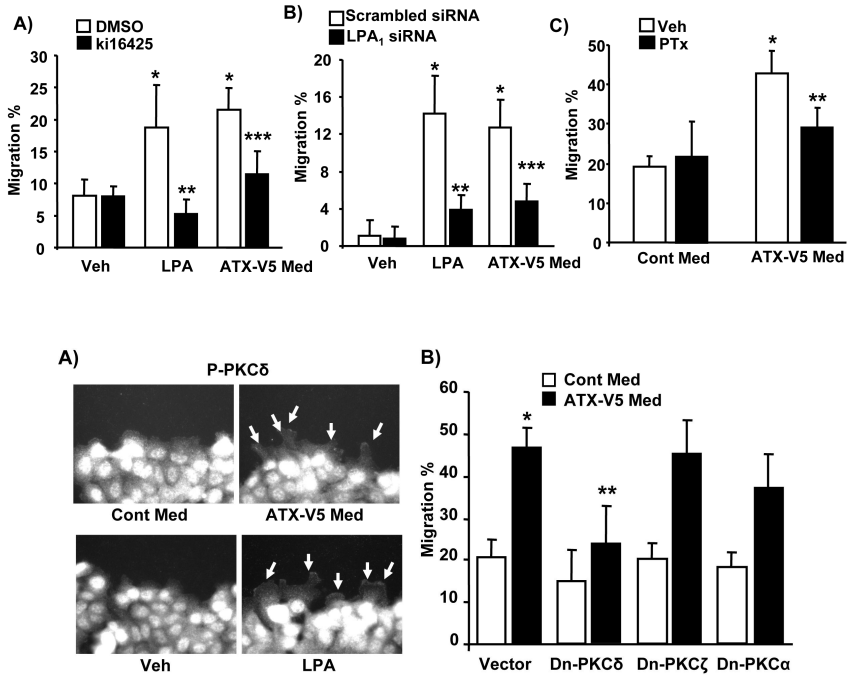

Figure 4. ATX-V5 Med increases cell migration through LPA_1 receptor

A) A549 cells were incubated with ki16425 (10 μM) for 1 h prior to LPA (1 μM) treatment or ATX-V5 Med incubation (18 h), and cell migration was measured by the scratch assay. The data represents mean ± S.D. from three independent experiments. *p<0.05, compared to veh; **p<0.05, compared to LPA alone; ***p<0.05, compared to ATX-V5 Med alone. B) A549 cells were transfected with scrambled or LPA_1 siRNA for 72 h prior to LPA (1 μM) treatment or ATX-V5 Med incubation (18 h), and cell migration was measured by the scratch assay. The data represents mean- ± S.D. from three independent experiments. *p<0.05, compared to veh; **p<0.05, compared to LPA alone; ***p<0.05, compared to ATX-V5 Med alone. C) A549 cells were pretreated with PTx (100 ng/ml) for 4 h, and then incubated with LPA (1 μM) or ATX-V5 Med for 18 h, and cell migration was measured by the scratch assay. The data represents mean ± S.D. from three independent experiments.*p<0.05, compared to veh; **p<0.05, compared to ATX-V5 Med alone.

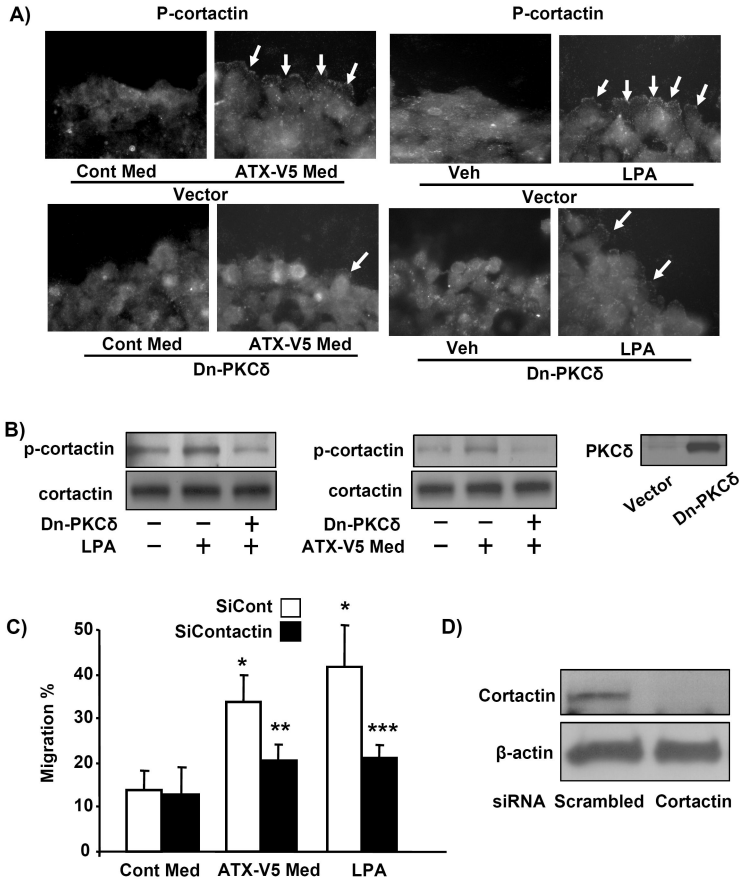

Figure 5. PKCδ regulates ATX-V5-induced cellular migration

A) A549 cells were scratched, and then were treated with ATX-V5 Med or LPA (1 μM) for 3 h. Immunostaining of phosphorylated PKCδ was performed using an antibody to p-PKCδ. Arrows indicate phospho-PKCδ. Also shown are representative images from three independent experiments. B) Cells were infected with Dn-PKCδ adenovirus or Dn-PKCζ or Dn-PKCα adenovirus (10 MOI) for 24 h, then cells were incubated with ATX-V5 Med and cell migration was measured by the scratch assay. The data represents mean ± S.D. from three independent experiments. *p<0.05, compared to Cont Med; **p<0.05, compared to ATX-V5 Med alone.

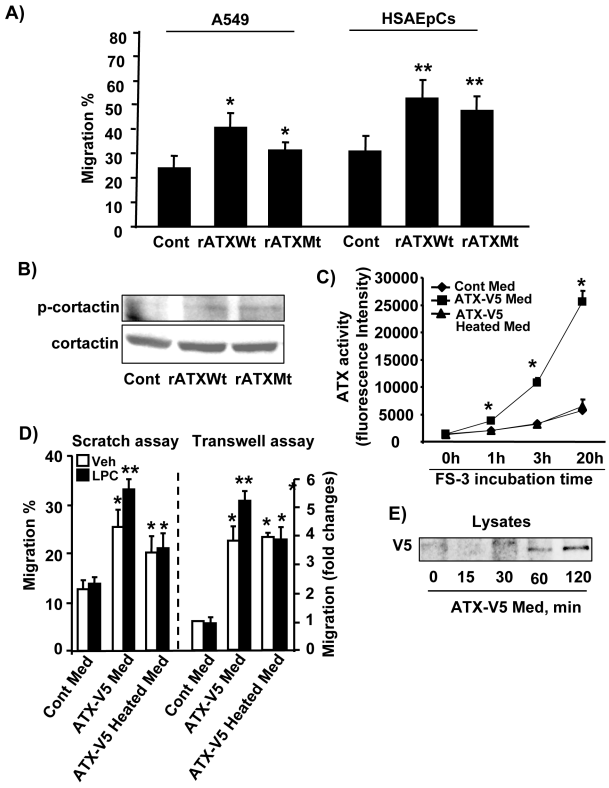

Figure 6. Cortactin regulates ATX-V5-induced cell migration

A) A549 cells were infected with Dn-PKCδ adenovirus (10 MOI) for 24 h, and then subjected to a scratch and incubated with ATX-V5 Med or LPA (1 μM) for 3 h. Cells were fixed and phosphorylated cortactin was immunostained using an antibody to p-cortactin. Arrows point to phospho-cortactin. Shown are representative images from three independent experiments. B) Cell lysates were analyzed by Western blotting with antibodies to cortactin, p-cortactin, and PKCδ. Shown are representative blots from three independent experiments. C) A549 cells were transfected with scrambled and cortactin siRNA (50 nM) for 72 h prior to incubation with ATX-V5 Med and LPA. Cell migration was measured by the scratch assay. The data represents mean ± S.D. from three independent experiments. *p<0.05, compared to veh; **p<0.05, compared to ATX-V5 medium alone; ***p<0.05, compared to LPA alone. D) Cell lysates were analyzed by immunoblotting with an antibody to cortactin. Shown are representative blots from three independent experiments.

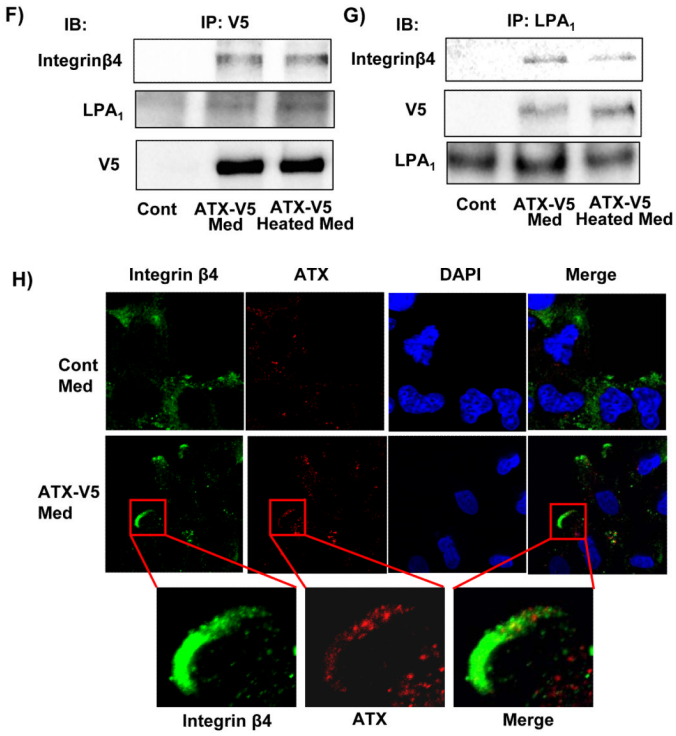

Figure 7. ATX complexes with LPA_1 and integrin β4

A) A549 and HSAEpCs cells were treated with recombinant ATX wild type (rATXWt) or ATX mutant (T210A) (rATXMt) for 18 h, and cell migration was measured by the scratch assay. The data represents mean ± S.D. from three independent experiments. *$p<0.05$, compared to A549 control; **$p<0.05$, compared to HSAEpCs control. B) A549 cells grown to 30 % confluence were treated with rATXWt or rATXMt for 3 h, cell lysates were analyzed by Western blotting with antibodies against phospho-cortactin and cortactin. Shown are representative blots from three independent experiments. C) ATX-V5 Med were heat-inactivated at 60 °C for 30 min, and ATX activities in ATX-V5 Med and ATX-V5 heat-inactivated Med were measured by using fluorescence FS-3 as substrate. The data represents mean ± S.D. from three independent experiments. *$p<0.01$, compared to Cont Med and ATX-V5 Heated Med. D) A549 cells were incubated with ATX-V5 Med or ATX-V5 heat-inactivated with or without egg LPC (50 μM) for 18 h and cell migration was measured by scratch and transwell invasion assay. The data represents mean ± S.D. pooled from three independent experiments. *$p<0.01$, compared to Cont Med. E) A549 cells were incubated with ATX-V5 Med for 15 - 120 min, and then subjected to 3 stringent washes. Cell lysates were analyzed by Western blotting with an antibody against V5 tag. A549 cells (~30 % confluent) were treated with ATX-V5 Med or ATX-V5 Heated Med for 3 h, and then stringently washed for at least four times. ATX-V5 (F) or LPA_1 (G) was immunoprecipitated from cell lysates with an antibody to V5 tag or LPA_1 separately and the immunoprecipitates were analyzed by Western blotting with antibodies to V5 tag, integrin β4, and LPA_1. Shown are representative blots from three independent experiments. H) A549 cells were treated with ATX-V5 Med for 3 h and fixed. Localization of integrin β4 and ATX were examined by antibodies to integrin β4 and ATX. Shown are representative images from three independent experiments.

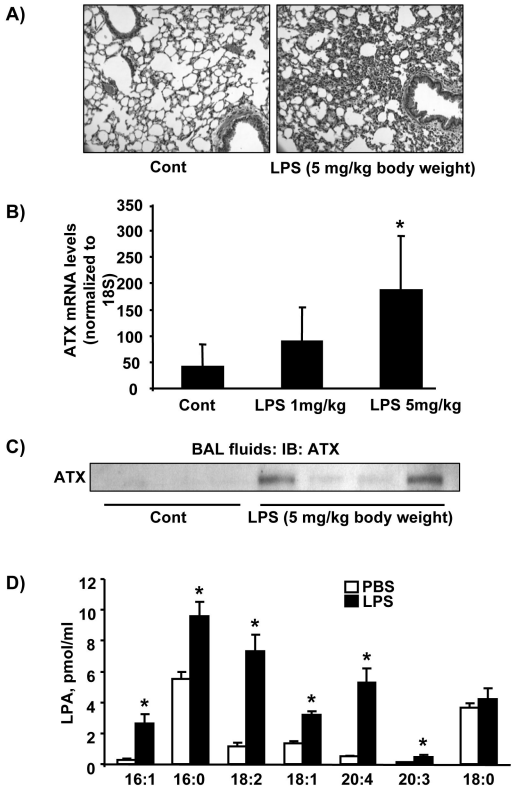

Figure 8. LPS increases ATX levels in lung fluid

A). Sv/129 mice were intratracheally challenged with PBS (n=3) or LPS (5 mg/kg body weight, n=4) for 24 h, and lung tissues were stained with H&E. Shown are representative images from 3-4 mouse tissues. B) Total RNA was extracted from lung tissue and ATX mRNA levels were measured by Real-time PCR. The data represents mean ± S.D. from 3-4 lung samples. C) BAL fluid from control and LPS challenged mice were analyzed by Western blotting with an antibody to ATX. Numbers indicate the number of mice used in each group. D) LPA levels in BAL fluids were measured by LC/MS/MS. The data represents mean ± S.D. from 3-4 samples. *<0.01, compared to PBS.

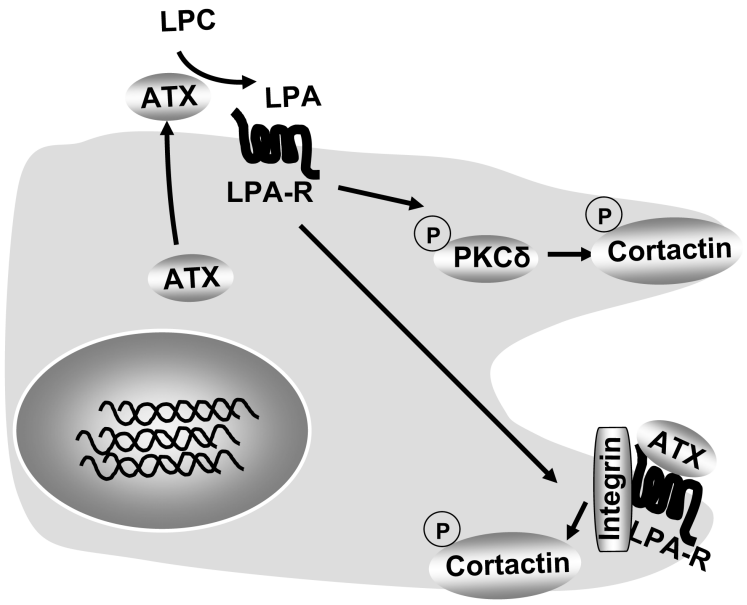

Figure 9. ATX regulates epithelial cell migration

Epithelial cells produce ATX that is released to outside. The two modalities of extracellular ATX mediated regulation of cell migration are: 1) LPA generation and LPA receptor-mediated activation of PKCδ and cortactin; and 2) ligation to LPA receptor and integrin on cell surface.

Table 1

ATX-V5 Med has lysoPLD activity.

	ATX-V5 Med				Heated-inactive ATX-V5 Med	
	0 μM LPC	**10 μM LPC**	**50 μM LPC**	**200 μM LPC**	**0 μM LPC**	**50 μM LPC**
16:1LPA	2.4±0.6	6.6±0.3	32.2±2.8	51.0±5.1	1.0±0.7	0.9±0.1
16:0LPA	7.0±1.3	52.9±9.4	369±22.9	559±65.6	6.9±4.3	0.0±0.0
18:2LPA	2.8±1.9	3.5±0.9	24.7±2.1	41.4±3.8	1.2±0.8	0.5±0.3
18:1LPA	9.2±2.9	12.1±1.8	61.7±4.8	92.5±8.5	2.8±0.9	3.4±0.7
18:0LPA	11.5±5.1	11.1±1.5	81.1±3.9	117.6±10.1	3.6±1.6	0.0±0.0
Total LPA	33.0±10.1	86.2±13.0	568±34.0	852±92.6	15.3±7.7	4.8±1.1

ATX-V5 Med and heated-inactive ATX-V5 Med were incubated with different concentration of egg LPC for 30 min. Lipids in the medium were then isolated and concentration of LPA species (fmol/ml) were measured by LC/MS/MS. The data represents mean± S.D. from three independent experiments.